A Dirichlet-to-Neumann Map Method for Second Harmonic Generation in Piecewise Uniform Waveguides

Lijun Yuan and Ya Yan Lu

Department of Mathematics, City University of Hong Kong
Kowloon, Hong Kong

For second harmonic generation in two-dimensional wave-guiding structures composed of segments that are invariant in the longitudinal direction, we develop an efficient numerical method based on the Dirichlet-to-Neumann (DtN) maps of the segments and a marching scheme using two operators and two functions. A Chebyshev collocation method is used to discretize the longitudinal variable for computing the DtN map and the locally generated second harmonic wave in each segment. The method rigorously solves the inhomogeneous Helmholtz equation of the second harmonic wave without making any analytic approximations. Numerical examples are used to illustrate this new method.

OCIS codes: 190.2620,130.2790,000.4430

1. Introduction

The nonlinear optical phenomenon of second harmonic generation (SHG) has found applications in many fields, such as laser fusion, biomedical instrumentation, femtosecond spectroscopy and precision metrology [1]. In a bulk medium, the second order nonlinear effect is typically very weak, unless there is a phase matching between the fundamental frequency and the second harmonic waves. In a number of applications, it is desirable to have SHG in optical waveguides. A practical way to improve the efficiency of SHG in waveguides is to include a periodic structure (possibly with defects) along the main propagation direction [2]. In this connection, SHG in waveguides that are piecewise uniform along the waveguide axis z has been studied numerically by a number of authors [3–6]. Efficient numerical methods are needed to analyze, design and optimize these structures. The finite difference time domain (FDTD) method has been generalized to study SHG [4], but frequency domain methods that take advantage of geometry features of the structure are often more efficient. To analyze linear waves in piecewise uniform waveguides, the eigenmode expansion methods [7–13]

and the bidirectional beam propagation methods (BiBPMs) [14–18] are particularly efficient. In a uniform segment, the eigenmode expansion methods allow us to avoid a discretization in the longitudinal variable z by expanding the wave field in the local eigenmodes of the segment. The BiBPMs are extensions of related methods for single waveguide discontinuities [19–23] and they can take full account of the multiple reflections at the longitudinal interfaces. The BiBPMs utilize the operator rational approximation techniques developed in traditional beam propagation method [24] for slowly varying waveguides to efficiently march the forward and backward wave field components in each uniform segment. In [5] and [6], the BiBPM and the eigenmode expansion method based on scattering operators are extended to analyze SHG, respectively. Both methods become rather complicated due to the inhomogeneous term in the governing equation of the second harmonic wave. For the eigenmode expansion method, when the second harmonic field in a uniform segment is expanded in the local eigenmodes, the coefficients are z dependent functions that can only be solved numerically. Both methods also make additional analytic approximations such as only co-propagating directional components are involved in the SHG process.

In a recent work [25], we developed an efficient method for linear waves in piecewise uniform waveguides based on the Dirichlet-to-Neumann (DtN) maps. For a uniform segment given by $z_{j-1} < z < z_j$, the DtN map M is an operator that maps the wave field at z_{j-1} and z_j to the z-derivative of the wave field there. The DtN map method is efficient, since computing the DtN map M is much easier than calculating the eigenmodes of the segment. To find M, we used a highly accurate Chebyshev collocation method to discretize z for the segment. Overall, the DtN map method is more efficient than the non-iterative BiBPM based on the scattering operators [16], and it is also more accurate since operator rational approximations used in the BiBPMs are mostly avoided. These rational approximants have difficulties to approximate both the propagating and the evanescent modes accurately. In this paper, we extend the DtN map method to SHG problems. It turns out that the DtN map method can easily handle the inhomogeneous term in the governing equation of the second harmonic wave without making any analytic approximations.

2. Problem formulation

We consider a two-dimensional (2D) wave-guiding structure in the xz plane and assume that both the fundamental frequency and second harmonic waves are given in the transverse electric (TE) polarization. Therefore, the y-component of the electric field is the real part of $ue^{-i\omega t} + ve^{-2i\omega t}$, where ω is the angular frequency of the fundamental frequency wave. The governing equations for SHG are

$$\partial_z^2 u + \partial_x^2 u + [k_0 n^{(1)}(x,z)]^2 u = -k_0^2 \chi^{(2)}(x,z)\, \bar{u} v, \tag{1}$$

$$\partial_z^2 v + \partial_x^2 v + [2k_0 n^{(2)}(x,z)]^2 v = -2k_0^2 \chi^{(2)}(x,z)\, u^2, \tag{2}$$

where $k_0 = \omega/c$ is the free space wavenumber, c is the speed of light in vacuum, $n^{(1)}$ and $n^{(2)}$ are the linear refractive index functions at ω and 2ω, respectively, $\chi^{(2)}$ is an element in the second order nonlinear susceptibility tensor. We assume that the structure is linear for $z < 0$ and $z > a$ and piecewise uniform (i.e., z-invariant) with longitudinal discontinuities at $z_0,\ z_1,\ \ldots,\ z_m$ satisfying $0 = z_0 < z_1 < \ldots < z_m = a$. For the segment (z_{j-1}, z_j), we have

$$\chi^{(2)}(x,z) = \chi_j^{(2)}(x), \quad n^{(l)}(x,z) = n_j^{(l)}(x), \quad l = 1, 2.$$

The above is valid even for $j = 0$ and $j = m+1$ if we define $z_{-1} = -\infty$ and $z_{m+1} = +\infty$. Notice that $\chi_0^{(2)} = \chi_{m+1}^{(2)} = 0$. For a given incident wave $u^{(i)}$ (at the fundamental frequency) in $z < 0$, we have transmitted waves in $z > a$ and reflected waves in $z < 0$ for both frequencies.

We can write down the boundary conditions at $z = 0$ and $z = a$ with properly defined square root operators. Let B_0 be the transverse operator of the fundamental frequency for $z < 0$, that is

$$B_0 = \partial_x^2 + [k_0 n_0^{(1)}(x)]^2.$$

The square root of B_0, denoted as $L_0^{(1)}$, can be defined as a linear operator satisfying $L_0^{(1)}\phi = \beta\phi$ for any eigenfunction ϕ and eigenvalue β^2 of the operator B_0 satisfying $B_0\phi = \beta^2\phi$. As the square root of β^2, the number β is chosen to satisfy $\mathrm{Im}(\beta) > 0$ or $\mathrm{Re}(\beta) > 0$ when $\mathrm{Im}(\beta) = 0$. This selection is based on our assumed time dependence $e^{-i\omega t}$ and it guarantees that $u = \phi e^{i\beta z}$ either decays as z is increased (an evanescent mode) or propagates in the increasing z direction. Since $L_0^{(1)}$ is defined as a linear operator, the principle of superposition applies. If a function f is expanded in the eigenfunctions of B_0, the action of $L_0^{(1)}$ on f can be evaluated by applying $L_0^{(1)}$ on each individual eigenfunctions linearly. With this definition, the incident wave and the reflected wave at the fundamental frequency satisfy

$$\partial_z u^{(i)} = iL_0^{(1)} u^{(i)}, \quad \partial_z u^{(r)} = -iL_0^{(1)} u^{(r)},$$

respectively. A boundary condition for the total field $u = u^{(i)} + u^{(r)}$ can be obtained if we eliminate the reflected wave $u^{(r)}$. We have

$$\partial_z u + iL_0^{(1)} u = 2iL_0^{(1)} u^{(i)}(x, 0-) \quad \text{at} \quad z = 0. \tag{3}$$

In general, we can define square root operators for all uniform segments and for both frequencies. For the segment (z_{j-1}, z_j), we have two square root operators for frequencies ω and 2ω, respectively:

$$L_j^{(l)} = \sqrt{\partial_x^2 + [lk_0 n_j^{(l)}(x)]^2}, \quad l = 1, 2.$$

Using the definitions, we arrive at the following boundary conditions:

$$\partial_z u - iL_{m+1}^{(1)} u = 0 \quad \text{at} \quad z = a, \tag{4}$$

$$\partial_z v + iL_0^{(2)} v = 0 \quad \text{at} \quad z = 0, \tag{5}$$

$$\partial_z v - iL_{m+1}^{(2)} v = 0 \quad \text{at} \quad z = a. \tag{6}$$

In principle, our problem is to solve the nonlinear coupled Helmholtz equations (1-2), subject to the boundary conditions (3-6).

Under the undepleted-pump approximation, the effect of the second harmonic wave on the fundamental frequency field is ignored. Eq. (1) is then replaced by the linear homogeneous Helmholtz equation:

$$\partial_z^2 u + \partial_x^2 u + [k_0 n^{(1)}(x,z)]^2 u = 0. \tag{7}$$

This approximation is appropriate for the examples considered in this paper. In principle, the method developed here can be used in an iterative procedure to solve the fully nonlinear SHG problem without the undepleted-pump approximation.

3. Marching scheme for second harmonic waves

A DtN operator marching method for u satisfying (7,3,4) was developed in [25]. The method relies on two operators that are approximated by matrices when the transverse variable x is discretized. These two operators are known at $z = a$ and they are marched from $z = a$ to $z = 0$. The step from z_j to z_{j-1} makes use of the DtN map of the segment. After we obtain these two operators at $z = 0$, we can find the reflected and transmitted waves.

In this section, we extend the DtN operator marching method to the inhomogeneous Helmholtz equation (2). In addition to the two operators, we also have to march two functions from $z = a$ to $z = 0$. These two functions are contributions of the the right hand side of (2). The operators Q_j, Y_j and functions $g_j(x)$, $f_j(x)$ are required to satisfy

$$Q_j\, v_j = \partial_z v_j - g_j, \tag{8}$$

$$Y_j\, v_j = v_m + f_j, \tag{9}$$

where v is an arbitrary solution of (2) and (6), $v_j = v(x, z_j)$, $v_m = v(x, a)$, $\partial_z v_j = \partial_z v(x, z_j)$. Condition (5) is excluded in the definition, thus the above equations are valid for infinitely many solutions of v. Furthermore, we insist that if the right hand side of (2) is zero, then $g_j = f_j = 0$ for all j. This implies that the operators Q_j and Y_j are defined independent of the inhomogeneous term. Therefore, they can be marched exactly the same way as described in [25]. When the transverse variable x is truncated and discretized by N points, Q_j and Y_j are approximated by $N \times N$ matrices, v_j, f_j and g_j are approximated by column vectors of length N.

From the boundary condition (6) and the definitions, we have

$$Q_m = iL_{m+1}^{(2)}, \quad g_m = 0, \quad Y_m = I, \quad f_m = 0, \tag{10}$$

where I is the identity operator. The square root operator $L_{m+1}^{(2)}$ can be evaluated by a rotating branch-cut Padé approximant. Next, we go through m steps as $j = m$, $m-1$, ...,

1. In the j-th step, we calculate Q_{j-1}, Y_{j-1}, f_{j-1} and g_{j-1} assuming that Q_j, Y_j, f_j and g_j are known. Once Q_0, Y_0, g_0 and f_0 are calculated, we can find the second harmonic waves at $z_0 = 0$ and $z_m = a$ from the boundary condition (5) and the definition (9). That is

$$\left[Q_0 + iL_0^{(2)}\right] v_0 = -g_0, \tag{11}$$

$$v_m = Y_0\, v_0 - f_0. \tag{12}$$

The square root operator $L_0^{(2)}$ above can be approximated by a rotating branch-cut Padé approximant. After that, we solve v_0 from (11) and evaluate v_m using (12).

For the step from z_j to z_{j-1}, we need the DtN map M and the locally generated second harmonic wave w of the segment. The operator M satisfies

$$M \begin{bmatrix} s(x, z_{j-1}) \\ s(x, z_j) \end{bmatrix} = \begin{bmatrix} M_{11} & M_{12} \\ M_{21} & M_{22} \end{bmatrix} \begin{bmatrix} s(x, z_{j-1}) \\ s(x, z_j) \end{bmatrix} = \begin{bmatrix} \partial_z s(x, z_{j-1}) \\ \partial_z s(x, z_j) \end{bmatrix}, \tag{13}$$

where $s = s(x, z)$ is an arbitrary solution of the homogeneous Helmholtz equation:

$$\partial_z^2 s + \partial_x^2 s + [2k_0 n_j^{(2)}(x)]^2 s = 0, \quad z_{j-1} < z < z_j. \tag{14}$$

The function w satisfies the inhomogeneous Helmholtz equation

$$\partial_z^2 w + \partial_x^2 w + [2k_0 n_j^{(2)}(x)]^2 w = -2k_0^2 \chi_j^{(2)}(x) u^2, \quad z_{j-1} < z < z_j \tag{15}$$

and zero Dirichlet boundary conditions $w = 0$ at $z = z_{j-1}$ and z_j. In section 4, we describe an efficient Chebyshev collocation method for calculating M and w. The marching formulas for the j-th step are

$$Z = (Q_j - M_{22})^{-1} M_{21}, \tag{16}$$

$$h = (Q_j - M_{22})^{-1} \left(g_j - \partial_z w|_{z_j}\right), \tag{17}$$

$$Q_{j-1} = M_{11} + M_{12} Z, \tag{18}$$

$$Y_{j-1} = Y_j Z, \tag{19}$$

$$g_{j-1} = \partial_z w|_{z_{j-1}} - M_{12} h, \tag{20}$$

$$f_{j-1} = Y_j h + f_j. \tag{21}$$

The formulas for Q_{j-1} and Y_{j-1} are identical to those given in [25], since they are unrelated to the inhomogeneous term in (2). The step involves linear systems with coefficient matrix $Q_j - M_{22}$ and matrix products $M_{12}Z$ and $Y_j Z$, etc. Therefore, this step requires $O(N^3)$ operations, where N is the number of points for discretizing x.

To derive the marching formulas, we assume that a solution v of the Helmholtz equation (2) satisfying the boundary condition (6) is written as $v = w + s$ in the segment (z_{j-1}, z_j), where

s satisfies the homogeneous equation (14) and w is the locally generated second harmonic wave. Meanwhile, we can evaluate $\partial_z v$ at z_{j-1} and z_j through (8), as well as through $v = w+s$ and the DtN map M for s. This gives rise to

$$\begin{aligned}(M_{11} - Q_{j-1})v_{j-1} + M_{12}v_j &= g_{j-1} - \partial_z w|_{z_{j-1}},\\ M_{21}v_{j-1} + (M_{22} - Q_j)v_j &= g_j - \partial_z w|_{z_j}.\end{aligned}$$

These two equations lead to

$$v_j = Zv_{j-1} - h, \tag{22}$$

$$(M_{11} - Q_{j-1} + M_{12}Z)v_{j-1} = g_{j-1} - \partial_z w|_{z_{j-1}} + M_{12}h. \tag{23}$$

Since (23) is supposed to be valid for all solutions of (2) and (6), it is necessary to require that Q_{j-1} satisfies (18) so that the left hand side is always zero. Formula (20) for g_{j-1} is obtained from the right hand side of (23). Furthermore, from (22) and (9) for j and $j-1$, we obtain

$$(Y_{j-1} - Y_j Z)v_{j-1} = f_{j-1} - f_j - Y_j h. \tag{24}$$

This gives rise to (19) and (21).

4. Chebyshev collocation method for uniform segments

The marching method described in the previous section relies on the DtN map M and the locally generated second harmonic wave w for each uniform segment. In [25], we developed a Chebyshev collocation method for calculating M using $O(qN^2)$ operations, where q is the number of points used to discretize z in the segment, i.e., $z_{j-1} < z < z_j$, and N is the number of points to discretize x. Since the Chebyshev collocation method has a very high accuracy for smooth functions, q is typically much smaller than N. Therefore, computing M is much easier than calculating the eigenmodes of the transverse operator. When x is discretized, the transverse operator is approximated by an $N \times N$ matrix. The eigenvalues and eigenvectors of this matrix can be calculated using $O(N^3)$ operations, but the constant hidden in the big O notation is quite large. In this section, the Chebyshev collocation method is used to find the locally generated second harmonic wave w. The required number of operations is only $O(q^2N)$.

For the segment (z_{j-1}, z_j), we discretize z by

$$\xi_k = z_{j-1} + \frac{z_j - z_{j-1}}{2}\left[1 - \cos\left(\frac{k\pi}{q}\right)\right], \quad k = 0, 1, ..., q. \tag{25}$$

Notice that $\xi_0 = z_{j-1}$ and $\xi_q = z_j$. Let F be a differential function of z, then the derivative

of F at ξ_k can be approximated by

$$\begin{bmatrix} F'(\xi_0) \\ F'(\xi_1) \\ \vdots \\ F'(\xi_q) \end{bmatrix} \approx C \begin{bmatrix} F(\xi_0) \\ F(\xi_1) \\ \vdots \\ F(\xi_q) \end{bmatrix}.$$

Here, C is the differentiation matrix [26] whose (k,l) entry (for $0 \le k,l \le q$) is given by

$$c_{kl} = -\frac{2}{z_j - z_{j-1}} \times \begin{cases} (2q^2+1)/6 & \text{if } k = l = 0, \\ -(2q^2+1)/6 & \text{if } k = l = q, \\ -0.5\tau_k/(1-\tau_k^2) & \text{if } 0 < k = l < q, \\ (-1)^{k+l}\sigma_k \sigma_l^{-1}/(\tau_k - \tau_l) & \text{otherwise,} \end{cases}$$

where

$$\tau_k = \cos\left(\frac{k\pi}{q}\right), \quad \sigma_k = \begin{cases} 2 & \text{if } k = 0,\, q \\ 1 & \text{if } 0 < k < q. \end{cases}$$

Naturally, the matrix C^2 gives approximations to the second order derivative of F. Let us write down C and C^2 as follows:

$$C = \begin{bmatrix} c_{00} & \tilde{c}_0 & c_{0q} \\ \vdots & \vdots & \vdots \\ c_{q0} & \tilde{c}_q & c_{qq} \end{bmatrix}, \quad C^2 = \begin{bmatrix} d_{00} & \cdots & d_{0q} \\ \hat{d}_0 & \hat{D} & \hat{d}_q \\ d_{q0} & \cdots & d_{qq} \end{bmatrix},$$

where $\tilde{c}_0$ and $\tilde{c}_q$ are row vectors, $\hat{d}_0$ and $\hat{d}_q$ are column vectors, and $\hat{D}$ is a square matrix. For the purpose of computing the DtN map M and the locally generated second harmonic wave w, we need to diagonalize $\hat{D}$:

$$\hat{D} = R \begin{bmatrix} \mu_1 & & & \\ & \mu_2 & & \\ & & \ddots & \\ & & & \mu_{q-1} \end{bmatrix} R^{-1}. \tag{26}$$

Meanwhile, we also need the following auxiliary vectors:

$$\vec{\alpha} = R^{-1}\hat{d}_0, \quad \vec{\beta} = R^{-1}\hat{d}_q, \quad \vec{\gamma} = \tilde{c}_0 R, \quad \vec{\delta} = \tilde{c}_q R. \tag{27}$$

The DtN map M defined in (13) can be obtained by repeatedly solving the homogeneous Helmholtz equation (14) for different choices of the boundary values, i.e, s at z_{j-1} and z_j. Due to a simple reflection symmetry, we have $M_{11} = -M_{22}$ and $M_{12} = -M_{21}$. Therefore, when x is discretized by N points, we can calculate M, as a $(2N)\times(2N)$ matrix, by choosing $[s(x, z_{j-1}), s(x, z_j)]^T$ in (13) as the first N column vectors of the $(2N)\times(2N)$ identity matrix. It turns out that for each choice of its boundary values, s satisfying (14) can be solved in

$O(qN)$ operations using the Chebyshev collocation method. Therefore, the DtN map can be constructed in $O(qN^2)$ operations. In the Chebyshev collocation method, we use C^2 to approximate ∂_z^2 in (14) and require that the equation is exactly valid at ξ_k for $1 \le k < q$. That is

$$\hat{d}_0 s_0 + \hat{D} \begin{bmatrix} s_1 \\ s_2 \\ \vdots \\ s_{q-1} \end{bmatrix} + \hat{d}_q s_q + \begin{bmatrix} Bs_1 \\ Bs_2 \\ \vdots \\ Bs_{q-1} \end{bmatrix} = \vec{0},$$

where $s_k = s(x, \xi_k)$ and $B = \partial_x^2 + [2k_0 n_j^{(2)}(x)]^2$ is the transverse operator. Assuming that $\hat{D}$ can be diagonalized as in (26), we can reduce the above to $q-1$ uncoupled ordinary differential equations:

$$\frac{d^2 p_k}{dx^2} + \left\{ [2k_0^2 n_j^{(2)}]^2 + \mu_k \right\} p_k = -\alpha_k s(x, z_{j-1}) - \beta_k s(x, z_j), \quad 1 \le k < q, \tag{28}$$

where $p_k = p_k(x)$ is given by

$$\begin{bmatrix} p_1 \\ p_2 \\ \vdots \\ p_{q-1} \end{bmatrix} = R^{-1} \begin{bmatrix} s_1 \\ s_2 \\ \vdots \\ s_{q-1} \end{bmatrix}.$$

The z-derivative of s can be evaluated using the matrix C. That is,

$$\partial_z s_0 = c_{00}\, s_0 + \tilde{c}_0 \begin{bmatrix} s_1 \\ s_2 \\ \vdots \\ s_{q-1} \end{bmatrix} + c_{0q}\, s_q.$$

Since $s_0 = s(x, z_{j-1})$ and $s_q = s(x, z_j)$, the above gives rise to

$$\partial_z s(x, z_{j-1}) = c_{00}\, s(x, z_{j-1}) + \sum_{k=1}^{q-1} \gamma_k p_k(x) + c_{0q}\, s(x, z_j). \tag{29}$$

Similarly, we have

$$\partial_z s(x, z_j) = c_{q0}\, s(x, z_{j-1}) + \sum_{k=1}^{q-1} \delta_k p_k(x) + c_{qq}\, s(x, z_j). \tag{30}$$

When x is discretized by N points and Eq. (28) is approximated by a finite difference or finite element method, we can solve p_k in $O(N)$ operations. Thus, $O(qN)$ operations are needed to find p_1, p_2, ..., p_{q-1}. Furthermore, the z-derivative of s at z_{j-1} and z_j can be calculated from (29) and (30) using $O(qN)$ operations. Therefore, one boundary value problem of (14) can be solved in $O(qN)$ operations. To construct the DtN map, we need to solve N boundary

value problems, so the required number of operations is $O(qN^2)$. The diagonalization of $\hat{D}$ requires $O(q^3)$ operations. Since q is much smaller than N, this is not significant compared with the other calculations.

Using the Chebyshev collocation method, we can solve the locally generated second harmonic wave w in $O(q^2N)$ operations. The function w satisfies the inhomogeneous Helmholtz equation (15) and zero boundary conditions at z_{j-1} and z_j. Using C^2 to approximate ∂_z^2 and assuming that (15) is satisfied at ξ_k for $1 \le k < q$, we have

$$\hat{D}\begin{bmatrix} w_1 \\ w_2 \\ \vdots \\ w_{q-1} \end{bmatrix} + \begin{bmatrix} Bw_1 \\ Bw_2 \\ \vdots \\ Bw_{q-1} \end{bmatrix} = -2k_0^2\chi_j^{(2)}(x)\begin{bmatrix} u^2(x,\xi_1) \\ u^2(x,\xi_2) \\ \vdots \\ u^2(x,\xi_{q-1}) \end{bmatrix},$$

where $w_k = w(x,\xi_k)$ and B is the transverse operator given earlier. The above can be transformed to

$$\frac{d^2r_k}{dx^2} + \left\{[2k_0^2n_j^{(2)}]^2 + \mu_k\right\} r_k = -2k_0^2\chi_j^{(2)}(x)\rho_k(x), \quad 1 \le k < q, \tag{31}$$

where

$$\begin{bmatrix} r_1 \\ r_2 \\ \vdots \\ r_{q-1} \end{bmatrix} = R^{-1}\begin{bmatrix} w_1 \\ w_2 \\ \vdots \\ w_{q-1} \end{bmatrix}, \quad \begin{bmatrix} \rho_1(x) \\ \rho_2(x) \\ \vdots \\ \rho_{q-1}(x) \end{bmatrix} = R^{-1}\begin{bmatrix} u^2(x,\xi_1) \\ u^2(x,\xi_2) \\ \vdots \\ u^2(x,\xi_{q-1}) \end{bmatrix}.$$

Finally, the z-derivative of w can be evaluated from:

$$\partial_z w(x,z_{j-1}) = \sum_{k=1}^{q-1}\gamma_k r_k(x), \quad \partial_z w(x,z_j) = \sum_{k=1}^{q-1}\delta_k r_k(x)$$

In the discrete case, ρ_1, ρ_2, ..., ρ_{q-1} are column vectors and they can be calculated using $O(q^2N)$ operations, the functions r_1, r_2, ..., r_{q-1} can be solved numerically from (31) using $O(qN)$ operations, and the z-derivative of w at z_{j-1} and z_j can be evaluated using $O(qN)$ operations. Therefore, the total number of operations required for computing w is $O(q^2N)$.

5. Numerical examples

To validate and illustrate our method, we consider two numerical examples. The first example has been analyzed by Locatelli *et al.* in [5]. It is a two-dimensional model (top view) of a deeply etched waveguide with a semiconductor core. Starting from a symmetric slab waveguide with air claddings and a core of width 2.5 μm, we introduce eight equally spaced air gaps in the waveguide core. The length of these air gaps is 0.2 μm. There are seven guiding segments between the air gaps. The length of each guiding segment is 0.837 μm. More precisely, we have

$$z_{2k} = 1.037\,k\,(\mu m), \quad z_{2k+1} = 1.037\,k + 0.2\,(\mu m), \quad \text{for} \quad k = 0, 1, ..., 7.$$

The total length of the z-varying part of the structure is $a = z_{15} = 7.459$ μm. In the waveguide core, we have a refractive index $n^{(1)} = 3.15$ at the fundamental frequency and $n^{(2)} = 3.3$ for the second harmonic. In our notation, these two values correspond to $n_{2k}^{(l)}(x)$ for $|x| < 1.25$ μm, $l = 1, 2$ and $0 \le k \le 8$. The second order nonlinear coefficient is assumed to be $\chi_{2k}^{(2)}(x) = 300$ pm/V in the waveguide core ($|x| < 1.25$ μm) for the seven guiding segments ($1 \le k \le 7$). Notice that $\chi^{(2)}$ is assumed to be zero for $z < 0$ and $z > a$. The incident wave is the fundamental mode of the original symmetric slab waveguide with a maximum electric field amplitude of 10^6 V/m.

In Fig. 1, we show the linear transmission and reflection properties of this structure around

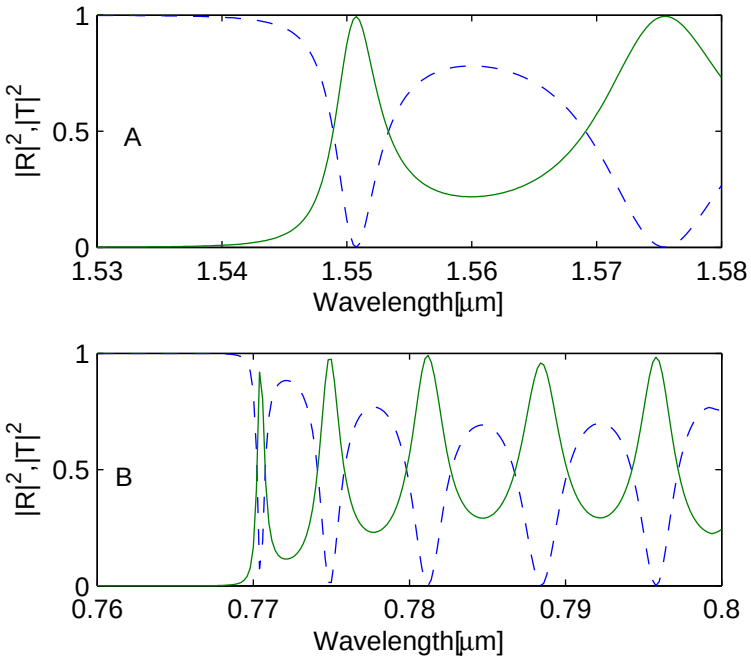

Fig. 1. Linear transmission and reflection properties of a piecewise uniform waveguide (Example 1) for two wavelength intervals. The solid and dashed lines represent $|T|^2$ and $|R|^2$, respectively.

the fundamental frequency and second harmonic wavelengths. The refractive index of the waveguide core is fixed at 3.15 for plot A and 3.3 for plot B, but there is no difficulty to use a more realistic dispersion model. The vertical axes show $|R|^2$ and $|T|^2$, where R and T are the amplitude reflection and transmission coefficients. We observe that the first transmission resonance around 1.55 μm in plot A matches well with the second transmission peak around 0.775 μm in plot B. We have calculated the second harmonic field for a number

of wavelengths. The maximum absolute value of the generated second harmonic wave at $z = a$ is shown versus the free space wavelength λ at the fundamental frequency in Fig. 2. At

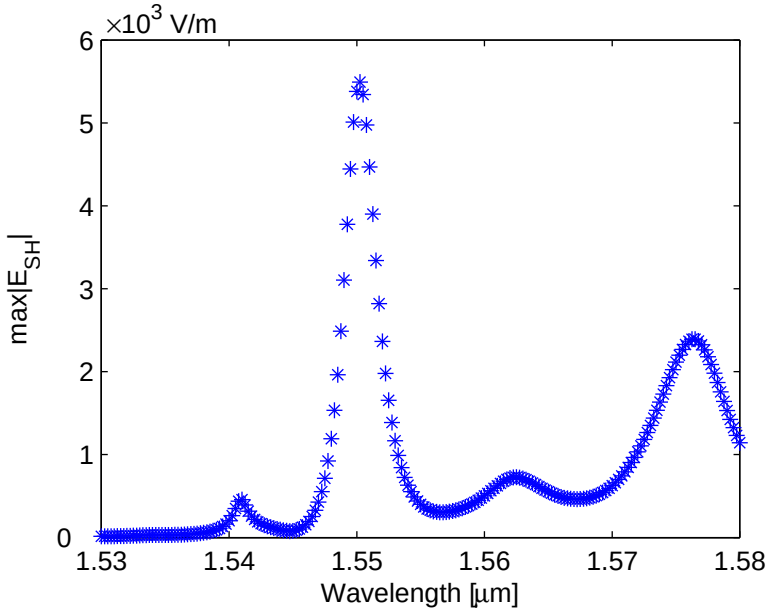

Fig. 2. Maximum amplitude of the generated second harmonic wave at $z = a$ for Example 1.

$\lambda = 1.55$ μm, the maximum we obtained is 5.37×10^3 V/m. This is slightly larger than the value 5.1×10^3 V/m reported in [5]. The magnitudes of the fundamental frequency and the second harmonic waves are shown (again for $\lambda = 1.55$ μm) in Fig. 3 and Fig. 4, respectively. Our numerical results are obtained with $q = 35$ for the guiding segments and $q = 10$ for the air gaps. The x variable is discretized form -2.5 μm to 2.5 μm with 201 points. Perfectly matched layers are used at the two ends of the interval.

The second example can be regarded as the side view of a three-dimensional deeply etched waveguide. The original z-invariant structure is a 2D slab waveguide with an air cladding and a non-dispersive substrate. The width of the waveguide core is $d = 3$ μm and the refractive index of the substrate is 3.1779. The z-varying part of the waveguide includes 11 air gaps of length 0.126 μm and depth $H = 4$ μm as shown in Fig. 5. Since $H > d$, the air gaps actually cut into the substrate. There are 10 guiding segments between the air gaps. The length of each guiding segment is 0.6 μm. This gives rise to

$$z_{2k} = 0.726\,k \ (\mu m), \quad z_{2k+1} = 0.726\,k + 0.126 \ (\mu m), \quad k = 0, 1, ..., 10.$$

The z-varying part of the structure starts at $z_0 = 0$ and ends at $z_{21} = a = 7.386\,\mu$m. The refractive index of the core is given by $n^{(1)} = 3.28$ and $n^{(2)} = 3.3815$ at the fundamental

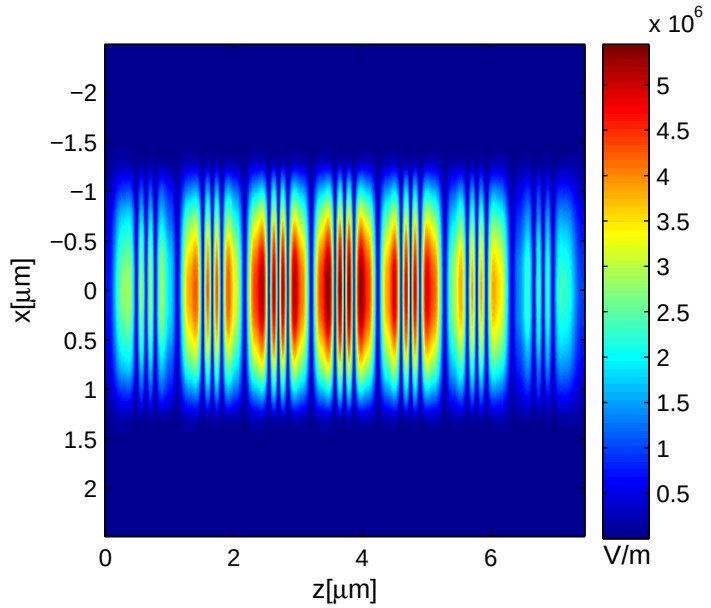

Fig. 3. Magnitude of the fundamental frequency wave for Example 1.

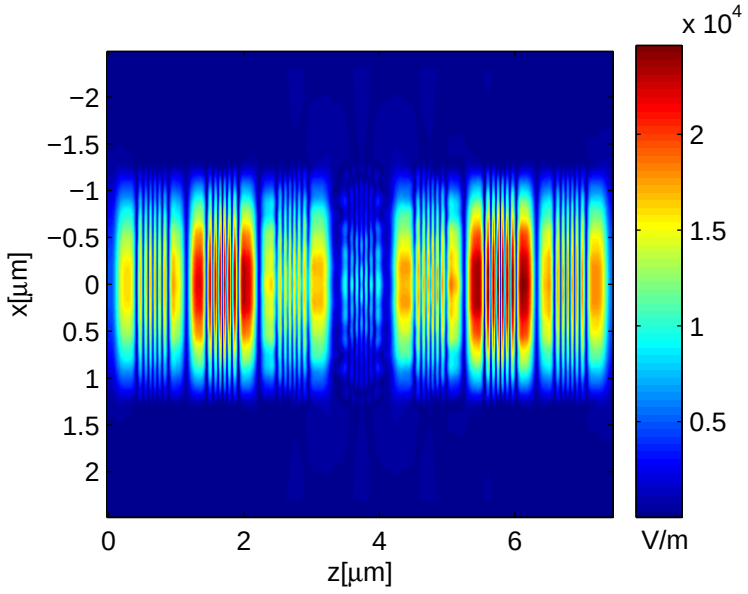

Fig. 4. Magnitude of the second harmonic wave for Example 1.

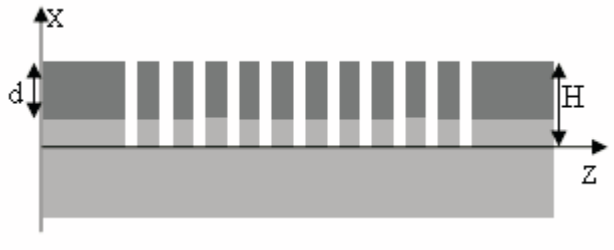

Fig. 5. A schematic view of the wave-guiding structure for Example 2.

and second harmonic frequencies. Only the waveguide core in the 10 guiding segments is assumed to be nonlinear and the second order nonlinear coefficient is $\chi^{(2)} = 240$ pm/V. For SHG, we assume that the incident wave $u^{(i)}$ is the fundamental propagating mode of the straight waveguide with a maximum amplitude of 10^6 V/m. In Fig. 6, we show the linear transmission and reflection properties of the structure. The refractive index of the core is assumed to a constant for all frequencies in each plot. That is, $n^{(1)} = 3.28$ and $n^{(2)} = 3.3815$ for plot A and B, respectively. The reflection and transmission coefficients R and T are those defined for field amplitudes. The structure is tuned to have a transmission peak at $1.55\,\mu$m for the fundamental frequency field and another transmission peak around $0.775\,\mu$m for the second harmonic field. The maximum amplitude of the generated second harmonic wave at the end of the z-varying part of the structure (i.e., $z = a$) is shown Fig. 7 as a function of the free space wavelength of the fundamental frequency wave. The largest second harmonic wave is obtained at the desired pump wave length $\lambda = 1.55\,\mu$m. In these calculations, we have discretized the transverse variable x from form $-1\,\mu$m to $5\,\mu$m with 251 points. In the z direction, the guiding segments and the air gaps are discretized by $q = 25$ and $q = 10$ points, respectively.

6. Conclusions

We have developed a marching scheme for second harmonic generation (SHG) in piecewise uniform waveguides based on Dirichlet-to-Neumann (DtN) maps. It is an extension of our earlier work [25] for linear waves. Due to an inhomogeneous term in the governing Helmholtz equation of the second harmonic wave, existing methods for SHG require additional analytic approximations. Our method solves the inhomogeneous Helmholtz equation rigorously. Compared with the linear DtN map method, the additional effort required for computing SHG is insignificant. The total required number of operations for computing the second harmonic wave in a structure with m segments is $O(mN^3)$, where N is the number of points for discretizing the transverse variable. To take advantage of the piecewise uniform nature

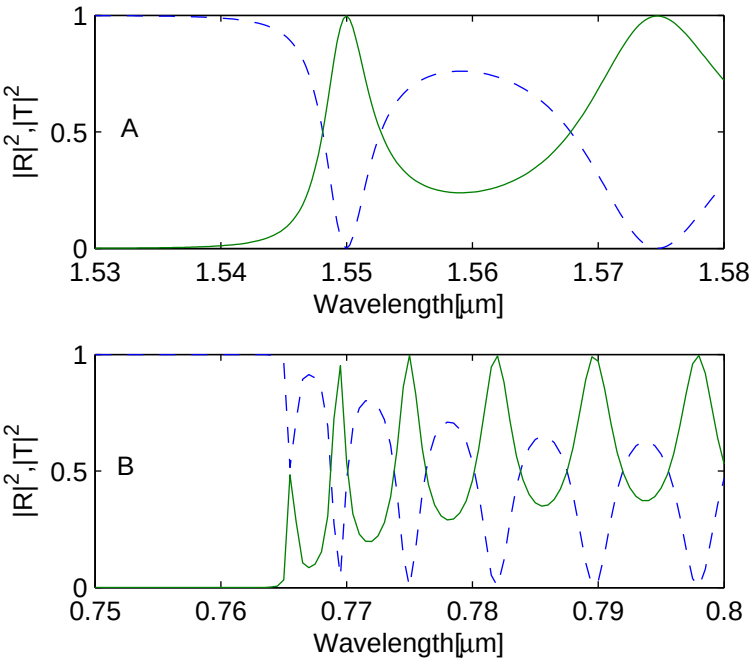

Fig. 6. Linear transmission and reflection properties of the piecewise uniform structure in Example 2. The solid and dashed lines represent $|T|^2$ and $|R|^2$, respectively.

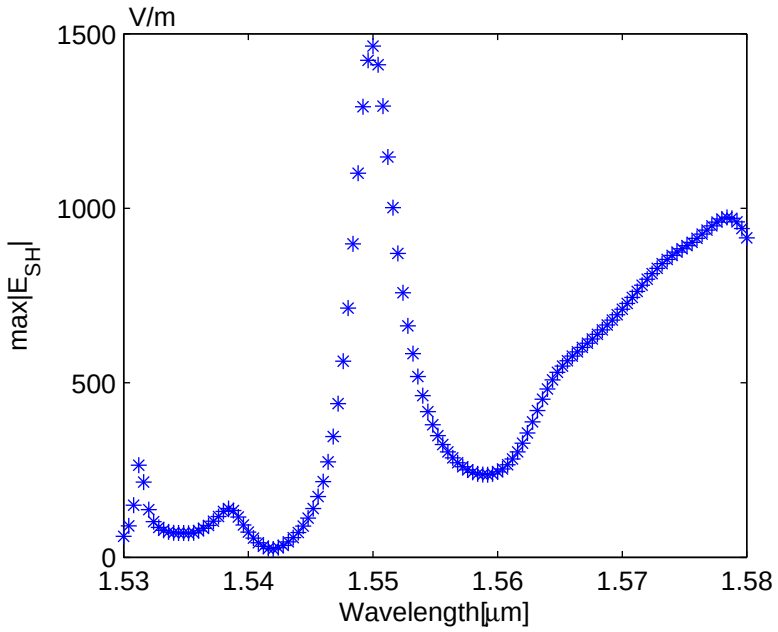

Fig. 7. The maximum amplitude of the generated second harmonic wave at $z = a$ versus the free space wavelength of the fundamental frequency, for Example 2

.

of the structure, a highly accurate Chebyshev collocation method is used to discretize z in each segment for computing the DtN map and the locally generated second harmonic field.

Acknowledgments

This research was partially supported by a grant from the Research Grants Council of Hong Kong Special Administrative Region, China (Project No. CityU 101706).

Lijun Yuan's e-mail address is 50008210@student.cityu.edu.hk. Ya Yan Lu's e-mail address is mayylu@cityu.edu.hk.

References

1. M. M. Fejer, "Nonlinear optical frequency conversion", *Physics Today*, Vol. 47, pp. 25-32, 1994.
2. M. Bertolotti, "Wave interations in photonic band structures: an overview", *J. Opt. A: Pure Appl. Opt.*, Vol. 8, pp. S9-S32, 2006.
3. W. Nakagawa, R. C. Tyan and Y. Fainman, "Analysis of enhanced second-harmonic generation in periodic nanostructures using modified rigorous coupled-wave analysis in the undepleted-pump approximation", *J. Opt. Soc. Am. A* , Vol. 19, pp. 1919-1928, 2002.
4. Y. Dumeige, F. Raineri, A. Levenson and X. Letartre, "Second-harmonic generation in one-dimensional photonic edge waveguides", *Phys. Rev. E* , Vol. 68, 066617, 2003.
5. A. Locatelli, D. Modotto, C. De Angelis, F. M. Pigozzo and A. D. Capobianco, "Nonlinear bidirectional beam propagation method based on scattering operators for periodic microstructured waveguides", *J. Opt. Soc. Am. B* , Vol. 20, pp. 1724-1731, 2003.
6. B. Maes, P. Bienstman and R. Baets, "Modeling second-harmonic generation by use of mode expansion", *J. Opt. Soc. Am. B*, Vol. 22, pp. 1378-1383, 2005.
7. Q. H. Liu and W. C. Chew, "Analysis of discontinuities in planar dielectric waveguides: an eigenmode propagation method", *IEEE Transactions on Microwave Theory and Techniques*, Vol. 39(3), pp. 422-430, March 1991.
8. G. Sztefka and H. P. Nolting, "Bidirectional eigenmode propagation for large refractive index steps", *IEEE Photonics Technology Letters*, Vol. 5, pp. 554-557, 1993.
9. J. Willems, J. Haes and R. Baets, "The bidirectional mode expansion method for 2-dimensional wave-guides - the TM case", *Optical and Quantum Electronics*, 27(10): 995-1007, Oct 1995.
10. S. F. Helfert and R. Pregla, "Efficient analysis of periodic structures", *Journal of Lightwave Technology*, Vol. 16, pp. 1694-1702, Sept. 1998.

11. P. Bienstman and R. Baets, "Optical modelling of photonic crystals and VCSELs using eigenmode expansion and perfectly matched layers", *Opt. Quant. Electron.*, Vol. 33, pp. 327-341, April 2001.
12. E. Silberstein, P. Lalanne, J. P. Hugonin and Q. Cao, "Use of grating theories in integrated optics", *J. Opt. Soc. Am. A*, Vol. 18, pp. 2865-2875, Nov. 2001.
13. J. Ctyroky, "A simple bi-directional mode expansion propagation algorithm based on modes of a parallel-plate waveguide", *Optical and Quantum Electronics*, 38 (1-3): 45-62, Jan. 2006.
14. H. Rao, R. Scarmozzino and R. M. Osgood, "A bidirectional beam propagation method for multiple dielectric interfaces", *IEEE Photonics Technology Letters*, Vol. 11, No. 7, pp. 830-832, 1999.
15. H. El-Refaei, D. Yevick and I. Betty, "Stable and noniterative bidirectional beam propagation method", *IEEE Photonics Technology Letters*, Vol. 12, pp. 389-391, 2000.
16. P. L. Ho and Y. Y. Lu, "A stable bidirectional propagation method based on scattering operators", *IEEE Photon. Technol. Lett.*, Vol. 13, No. 12, pp. 1316-1318, 2001.
17. P. L. Ho and Y. Y. Lu, "A bidirectional beam propagation method for periodic waveguides", *IEEE Photon. Technol. Lett.*, Vol. 14, pp. 325-327, March 2002.
18. Y. Y. Lu and S. H. Wei, "A new iterative bidirectional beam propagation method", *IEEE Photonics Technology Letters*, Vol. 14, No. 11, pp. 1533-1535, Nov. 2002.
19. Y. P. Chiou and H. C. Chang, "Analysis of optical waveguide discontinuities using the Padé approximations", *IEEE Photon. Technol. Lett.*, Vol. 9, pp. 946-966, 1997.
20. C. Yu and D. Yevick, "Application of the bidirectional parabolic equation method to optical waveguide facets", *J. Opt. Soc. Am. A*, Vol. 14, No. 7, pp. 1448-1450, 1997.
21. H. El-Refaei, I. Betty and D. Yevick, "The application of complex Padé approximants to reflection at optical waveguide facets", *IEEE Photon. Technol. Lett.*, vol. 12, no. 2, Feb. 2000.
22. S. H. Wei and Y. Y. Lu, "Application of Bi-CGSTAB to waveguide discontinuity problems", *IEEE Photon. Technol. Lett*, Vol. 14, pp. 645-647, 2002.
23. N. N. Feng and W. P. Huang, "A field-based numerical method for three-dimensional analysis of optical waveguide discontinuities", *IEEE J. Quantum Electronics*, Vol. 39, pp. 1661-1665, Dec. 2003.
24. J. Yamauchi, *Propagating Beam Analysis of Optical Waveguides*, Research Studies Press, UK, 2003.
25. L. Yuan and Y. Y. Lu, "An efficient bidirectional propagation method based on Dirichlet-to-Neumann maps", *IEEE Photon. Technol. Lett.*, Vol. 18, pp. 1967-1969, Sept. 2006.
26. L. N. Trefethen, *Spectral Methods in MATLAB*, Society for Industrial and Applied Mathematics, 2000.